Termination of Replication Stress Signaling via Concerted Action of the Slx4 Scaffold and the PP4 Phosphatase

Carolyn M. Jablonowski,*,[1] José R. Cussiol,*,[1] Susannah Oberly,* Askar Yimit,[†] Attila Balint,[†] TaeHyung Kim,[‡] Zhaolei Zhang,[‡] Grant W. Brown,[‡] and Marcus B. Smolka*,[2]

*Department of Molecular Biology and Genetics, Weill Institute for Cell and Molecular Biology, Cornell University, Ithaca, New York 14853, and [†]Donnelly Centre and Department of Biochemistry and [‡]Donnelly Centre and Department of Computer Science, University of Toronto, Toronto, Ontario, M5S 3E1, Canada

ORCID ID: 0000-0001-5909-8215 (J.R.C.)

ABSTRACT In response to replication stress, signaling mediated by DNA damage checkpoint kinases protects genome integrity. However, following repair or bypass of DNA lesions, checkpoint signaling needs to be terminated for continued cell cycle progression and proliferation. In budding yeast, the PP4 phosphatase has been shown to play a key role in preventing hyperactivation of the checkpoint kinase Rad53. In addition, we recently uncovered a phosphatase-independent mechanism for downregulating Rad53 in which the DNA repair scaffold Slx4 decreases engagement of the checkpoint adaptor Rad9 at DNA lesions. Here we reveal that proper termination of checkpoint signaling following the bypass of replication blocks imposed by alkylated DNA adducts requires the concerted action of these two fundamentally distinct mechanisms of checkpoint downregulation. Cells lacking both *SLX4* and the PP4-subunit *PPH3* display a synergistic increase in Rad53 signaling and are exquisitely sensitive to the DNA alkylating agent methyl methanesulfonate, which induces replication blocks and extensive formation of chromosomal linkages due to template switching mechanisms required for fork bypass. Rad53 hypersignaling in these cells seems to converge to a strong repression of Mus81-Mms4, the endonuclease complex responsible for resolving chromosomal linkages, thus explaining the selective sensitivity of *slx4*Δ *pph3*Δ cells to alkylation damage. Our results support a model in which Slx4 acts locally to downregulate Rad53 activation following fork bypass, while PP4 acts on pools of active Rad53 that have diffused from the site of lesions. We propose that the proper spatial coordination of the Slx4 scaffold and PP4 action is crucial to allow timely activation of Mus81-Mms4 and, therefore, proper chromosome segregation.

KEYWORDS DNA damage checkpoint; Slx4; PP4; replication stress; Rad53

REPLICATION stress is one of the main sources of genomic instability that has been associated with the onset of cancers (Myung *et al.* 2001; Kastan and Bartek 2004; Branzei and Foiani 2009). To cope with stress during DNA replication, cells rely on the DNA damage checkpoint (DDC), a surveillance mechanism that senses abnormal DNA structures and elicits signaling responses that coordinate multiple cellular processes. With the goal of preserving genome integrity and cell viability, DDC signaling triggers cell cycle arrest (Weinert and Hartwell 1988), inhibition of replication origin firing (Santocanale and Diffley 1998; Zegerman and Diffley 2010), and replication fork protection mechanisms that include an increase of dNTP pools (Zhou and Elledge 1993; Zhao *et al.* 2001; Davidson *et al.* 2012) and inhibition of nucleases such as Exo1 (Morin *et al.* 2008). In *Saccharomyces cerevisiae*, the DDC is orchestrated mainly by the action of the apical PI3K-like kinase (PI3KK) Mec1 (ATR in humans) that senses the damage as exposure of single-stranded DNA (ssDNA) and transduces the signal to the downstream effector kinase Rad53 (human CHK2/CHK1), which will then enforce most of the responses that characterize a canonical DDC (Sanchez *et al.* 1996; Sun *et al.* 1996). A critical step in the activation of the DDC is the recruitment of Rad53 to sites of DNA lesions. While Mec1 is rapidly recruited to regions of ssDNA via a direct interaction of

doi: 10.1534/genetics.115.181479
Manuscript received July 31, 2015; accepted for publication September 9, 2015; published Early Online September 11, 2015.
Supporting information is available online at www.genetics.org/lookup/suppl/doi:10.1534/genetics.115.181479/-/DC1.
[1]These authors contributed equally to this work.
[2]Corresponding author: 339 Weill Hall, Cornell University, Ithaca, NY 14853-7202. E-mail: mbs266@cornell.edu

its cofactor Ddc2 with ssDNA-coated RPA (Zou and Elledge 2003), the recruitment of Rad53 is subject to extensive regulation and requires the involvement of DDC adaptors (a.k.a. mediators) Rad9 or Mrc1. Mrc1 is a component of the replisome and is mostly involved in recruiting Rad53 to stalled replication forks (Alcasabas *et al.* 2001). Rad9 mediates Rad53 recruitment and activation in response to a broader variety of DNA lesions, including double-strand breaks (DSBs) and DNA lesions induced by replication stress in which replication forks bypass the lesion, leaving ssDNA gaps behind (Sun *et al.* 1998; Gilbert *et al.* 2001; Schwartz *et al.* 2002; Branzei and Foiani 2010). Rad9 is recruited to DNA lesions by direct recognition of chromatin marks, including histone H2A phosphorylated at serine 129 (γ-H2A) and methylated histone H3K79 (Giannattasio *et al.* 2005; Grenon *et al.* 2007; Hammet *et al.* 2007), via its BRCT and Tudor domains, respectively. Rad9 is also recruited to DNA lesions via interaction with the Dpb11 scaffold, which binds to a Mec1-phosphorylated site in the 9-1-1 clamp loaded at ss/double-stranded DNA (ss/dsDNA) junctions (Puddu *et al.* 2008; Granata *et al.* 2010; Pfander and Diffley 2011). Recruitment of Rad9 via multiple partially redundant mechanisms is believed to increase opportunities for regulating Rad53 recruitment and activation, therefore helping to fine-tune DDC activation levels (Ohouo and Smolka 2012). Once Rad9 is recruited, it is extensively phosphorylated by Mec1, creating docking phospho-sites that are recognized by the forkhead-associated (FHA) domains of Rad53, enabling Rad53 to be recruited in the vicinity of Mec1 (Grenon *et al.* 2001; Schwartz *et al.* 2002; Sweeney *et al.* 2005). Mec1 then phosphorylates and activates Rad53, which undergoes further autophosphorylation in *trans* to reach its full activation state (Gilbert *et al.* 2001). Once activated, Rad53 is believed to quickly diffuse throughout the nucleus to phosphorylate its physiological substrates, eliciting a global checkpoint response (for review see Pellicioli and Foiani 2005).

Despite the key roles for Rad53 signaling in the replication stress response, it is imperative that its activity is precisely regulated. Because checkpoint signaling represses DNA replication and cell cycle progression, downregulation of Rad53 activity is essential for the resumption of cell proliferation once the DNA damage is repaired or bypassed. Although activation of DDC has been extensively studied, less is understood about its downregulation. The PP2C phosphatases, Ptc2 and Ptc3, were first characterized as important for Rad53 dephosphorylation and checkpoint recovery following DSB induction (Leroy *et al.* 2003). Later on, the PP4 phosphatase complex Pph3-Psy2 was shown to be important for Rad53 dephosphorylation following treatment with the DNA alkylating agent methyl methanesulfonate (MMS), which generates replication blocks that are readily bypassed by moving replication forks (O'Neill *et al.* 2007). In addition to phosphatase-mediated mechanisms, we have recently uncovered a new mechanism of Rad53 downregulation involving direct displacement of Rad9 from DNA lesions (Ohouo *et al.* 2013; Cussiol *et al.* 2015). In this phosphatase-independent mechanism, named **d**ampens **a**daptor-**m**ediated **p**hosphosignaling (DAMP), a complex formed by the DNA repair scaffolds Slx4 and Rtt107 competes with Rad9 by interacting with two proteins required for Rad9 recruitment, namely γ-H2A and Dpb11. As a consequence, Rad9 is displaced from DNA lesions, prohibiting further transduction of Mec1 signaling to Rad53, thus dampening the DDC. Interestingly, Slx4 has an established role as a scaffold for the coordination of structure-specific nucleases (Mullen *et al.* 2001; Rouse 2009), so the identification of a nuclease-independent function for Slx4 in DDC regulation suggests an intricate mechanism for the crosstalk and coordination of DDC signaling control and DNA repair.

Here we report that proper termination of DDC signaling following the bypass of replication blocks imposed by alkylated DNA adducts requires the concerted and highly complementary actions of Slx4 and the PP4 phosphatase. We find that cells lacking both *SLX4* and the *PPH3* subunit of PP4 display a synergistic increase in Rad53 signaling and are exquisitely sensitive to MMS. Rad53 hyperactivation in these mutants seems to indirectly converge to repression of Mus81-Mms4, a nuclease involved in the resolution of sister chromatid linkages that are byproducts of replication fork bypass events. Our results support a model in which Slx4-Rtt107 acts locally to downregulate Rad53 activation following fork bypass, while PP4 acts on free nuclear pools of active Rad53 to globally turn off the checkpoint response.

Materials and Methods

Yeast strains and plasmids

Strains generated in this study were derived from MBS164 or MBS191 (both congenic to S288C) or W303 (where indicated). All yeast strains and plasmids used in this study are described in Supporting Information, Table S1 and Table S2, respectively. Strains were constructed using standard genetic protocols for knockout and epitope tagging (Bähler *et al.* 1998; Longtine *et al.* 1998). All yeast transformations were performed using the lithium acetate method (Gietz *et al.* 1992). The yeast strain carrying the *rad53-R605A* allele was generated by linearizing a plasmid carrying *rad53-R605A-kanMX6* (pMBS 362) and integrating it at the endogenous *RAD53* locus. Integration was selected on rich medium (YPD) in the presence of G418 (300 μg/ml). Individual colonies were selected for DNA extraction and the *rad53-R605A* allele was confirmed by DNA sequencing.

Western blot analysis

Rad53 and phosphorylated histone H2A proteins were probed using specific antibodies: anti-Rad53 (clone Mab EL7, gift from Achille Pellicioli (Department of Biosciences, University of Milan, Milano, Italy), 1:30 dilution), anti-γ-H2A (Ab17353-Abcam, 1:5000 dilution), and ECL HRP-linked secondary antibody (NA931-GE, 1:10,000 dilution).

Cell cycle synchronization

Cells were grown in YPD medium at 30° until log phase. For arrest of cells in G_1, α-factor (Zymo Research) was added to a final concentration of 50 ng/ml (for *bar1Δ* background

strains) and incubated for 2 hr. To release cells from G_1 arrest, cells were centrifuged and resuspended in fresh medium in the presence of pronase [50 ng/ml, Sigma (St. Louis) P5147] and MMS (where indicated).

DNA damage sensitivity

Cells were grown until log phase, normalized to an optical density (OD) of 0.8. Fourfold serial dilutions were spotted on YPD or synthetic complete medium lacking uracil (SC –URA) plates and grown for 2–3 days at 30° in the presence or absence of drugs.

Flow cytometry

One milliliter of log-phase yeast cultures was collected, harvested, resuspended in 1 ml of 70% ethanol, and incubated for 15 min at room temperature or overnight at 4°. Cells were then centrifuged, supernatant was removed, and residual ethanol was dried in a speed-vac. After that, samples were solubilized in sodium citrate buffer (50 mM, pH 7.2) and sonicated (three cycles of 3 sec, amplitude 30%) to break up cell clumps. Samples were then incubated with 200 μg of RNAse A (QIAGEN, Valencia, CA) for 2 hr at 37° followed by incubation with 500 μg of Proteinase K (Invitrogen, Carlsbad, CA) for 1 hr at 42°. Finally, 1 μl of SYTOX Green (Life Technologies) was added to the samples and incubated for 2 hr at 4° protected from the light. Data were acquired using a BD Accuri C6 Flow Cytometer.

Pulsed-field gel electrophoresis

Cells were allowed to reach log phase in 200 ml of YPD medium. An untreated, asynchronous sample (ASY) was taken for control. Cells were then treated with MMS for 2 hr and then centrifuged and recovered in fresh, MMS-free medium for up to 6 hr. For a detailed protocol please see Cussiol *et al.* (2015).

Confocal fluorescence microscopy

Colocalization of Pph3-GFP and Slx4-yEmCherry was analyzed by growing yeast cultures (AYY183: *MAT***a** *SLX4-yEmCherry*::*CaURA3*, *Pph3-GFP*::*HIS3MX STE2pr-LEU2 lyp1Δ ura3Δ0 leu2Δ0 his3Δ1 met15Δ0*) to saturation in YPD, diluting them into fresh YPD to $OD_{600} = 0.1$, and growing them for 2 hr at 30° before treating them with 0.03% MMS. Eleven *z* slices with a 0.4-μm step size were acquired using Volocity imaging software (Perkin-Elmer, Norwalk, CT) controlling a Leica DMI6000 microscope with the fluorescein isothiocyanate, Texas Red and differential interference contrast filter sets (Quorum Technologies). Slx4-yEmCherry foci, Pph3-GFP foci, and colocalizing foci were counted in >500 cells total, in two independent experiments.

Chromatin immunoprecipitation and deep sequencing

Chromatin immunoprecipitation and deep sequencing (ChIP-seq) analysis was performed as previously described (Balint *et al.* 2015). Briefly, cells were synchronously released into 0.04% MMS for 60 min, cross-linked with formaldehyde, and subjected to chromatin immunoprecipitation. Sequencing libraries were generated from immunoprecipitated (IP) and input (IN) DNA, using the Nextera XT DNA Sample Preparation Kit (Illumina) with custom Index primers, and sequenced using the HiSequation 2500 (Illumina). Data are presented for chromosome 10 as a log2 ratio of normalized read counts for each IP:input pair. Enrichment values for 1-kb bins across 50 kb upstream and downstream of each replication origin were extracted to visualize median (±SE) protein enrichment across all early origins. Replication profiles were generated using VarScan 2 [version 2.3.5; default settings (Koboldt *et al.* 2012)] by comparing sequencing read counts from the input samples with sequencing read counts from a reference sample from a G_1-arrested strain (BY4741).

Data availability

All sequencing data are deposited in the Sequence Read Archive (http://www.ncbi.nlm.nih.gov/sra; Study accession SRP062915). Strains and plasmids are available upon request. Tables S1 and S2 contain the list of yeast strains and plasmids used in this study, respectively. Figure S1 contains supplemental data in support of Figure 2. Figure S2 contains supplemental data in support of Figure 3C.

Results

Cells lacking PPH3 or SLX4 display similar defects upon MMS-induced replication blocks

Rad53 is activated in response to a wide range of genotoxins and types of replication stress (Sun *et al.* 1996; Pellicioli *et al.* 1999). Notably, *pph3Δ* cells and *slx4Δ* cells display hypersensitivity to replication stress induced by the DNA alkylating agent MMS but not to replication stress induced by the ribonucleotide reductase (RNR) inhibitor hydroxyurea (HU) (Figure 1A). A distinct feature of MMS-induced DNA lesions is the extensive generation of adducts, mostly N7-guanine methylation on one of the DNA strands, which are readily bypassed by moving replication forks (Branzei and Foiani 2010). Upon exposure to MMS, both *pph3Δ* cells and *slx4Δ* cells display hyperactivation of Rad53 and an intra-S delay (Figure 1, B and C), consistent with previous reports (Chang *et al.* 2002; Roberts *et al.* 2006; O'Neill *et al.* 2007; Ohouo *et al.* 2013). Furthermore, both *pph3Δ* cells and *slx4Δ* cells exhibit MMS-induced chromosomal defects visualized by pulsed-field gel electrophoresis (PFGE) (Figure 1D) (see also Roberts *et al.* 2006 for *slx4Δ*), a defect often attributed to either incomplete chromosomal replication or improper processing of joint chromosomal structures (Hennessy *et al.* 1991; Saugar *et al.* 2013). Consistent with these findings, checkpoint signaling has been shown to counteract DNA replication, S-phase progression, and timely resolution of joint chromosomes (Santocanale and Diffley 1998; Szyjka *et al.* 2008; Szakal and Branzei 2013). Of importance, the MMS sensitivity of both *pph3Δ* cells and *slx4Δ* cells could be rescued by a hypomorphic allele of *RAD53* (*rad53-R605A*) that we have previously shown to lower Rad53 activation levels (Ohouo *et al.* 2013) (Figure 1E). Taken together, these results show that *pph3Δ* cells display similar

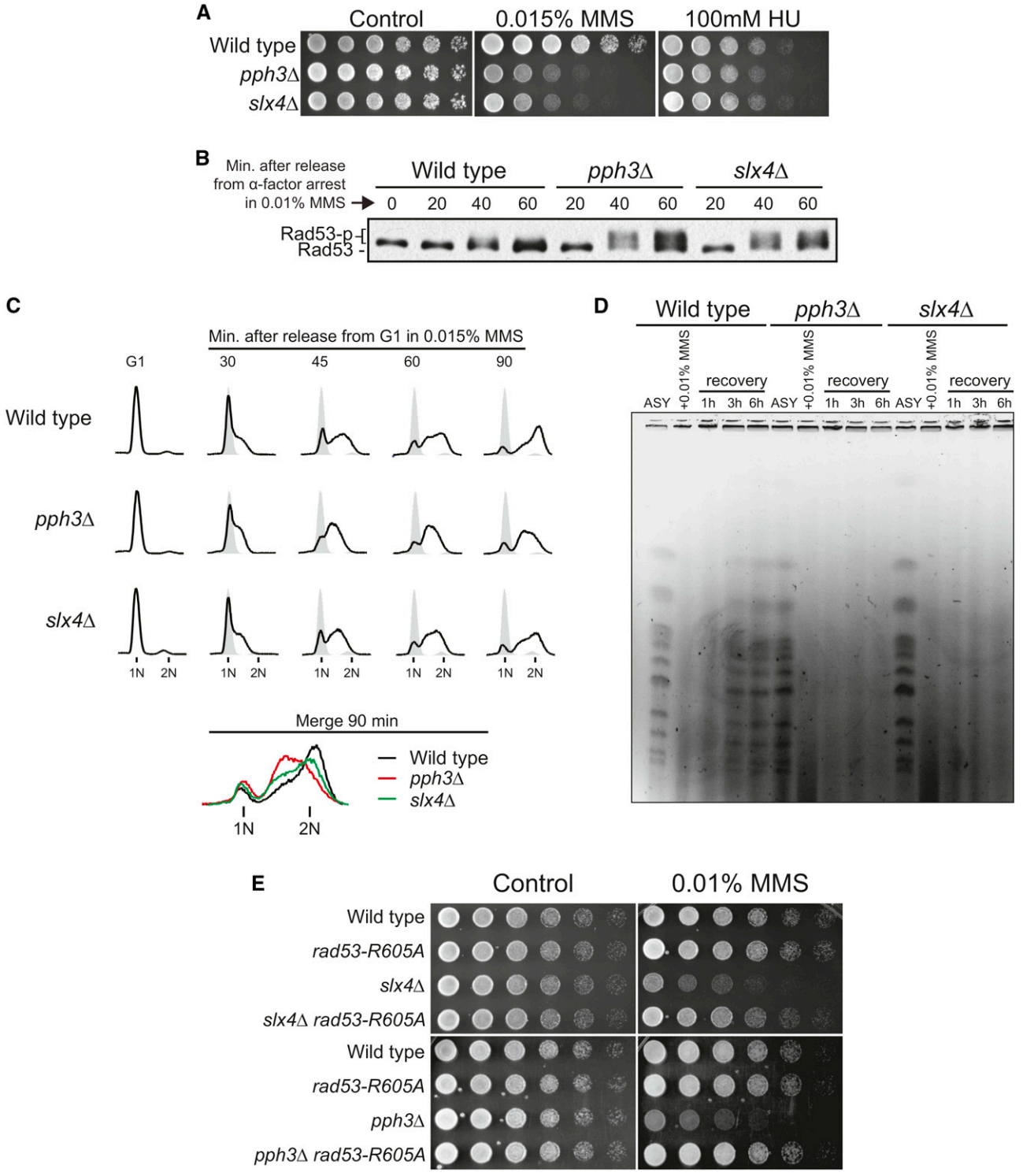

Figure 1 Cells lacking either *PPH3* or *SLX4* show similar defects upon replication stress induced by MMS. (A) Serial dilution assays showing the effect of genotoxin treatment upon the sensitivity of wild-type, *slx4Δ*, and *pph3Δ* cells. Fourfold serial dilutions were spotted on YPD plates and grown for 2–3 days at 30°. (B) Anti-Rad53 immunoblots of wild-type, *slx4Δ*, and *pph3Δ* strains showing Rad53 phosphorylation status after MMS treatment. (C) S-phase progression analysis of wild-type, *slx4Δ*, and *pph3Δ* strains. For B and C, cells were arrested in G_1 with α-factor and then released in medium containing MMS. Samples were collected in G_1 and at different time points following release. (D) Analysis of fully replicated chromosomes measured by PFGE in wild-type, *slx4Δ*, and *pph3Δ* strains. Asynchronous (ASY) cells were treated with 0.01% MMS for 2 hr and then released in MMS-free medium for up to 6 hr. (E) Serial dilution assay showing the effect of a hypomorphic *RAD53* allele (*rad53-R605A*) on MMS sensitivity of wild-type, *slx4Δ*, and *pph3Δ* strains.

defects to *slx4Δ* cells upon exposure to MMS-induced replication stress and that in both cases the observed defects are caused by improper regulation of Rad53 signaling.

Pph3 and Slx4 represent complementary mechanisms for Rad53 downregulation following MMS-induced replication stress

To better understand the functional interplay between the phosphatase-mediated (via Pph3) and the DAMP-mediated (via Slx4) mechanisms for Rad53 downregulation, we analyzed cells lacking both *PPH3* and *SLX4*. When compared to the single mutants, *pph3Δ slx4Δ* cells display a significant increase in Rad53 activation, which was accompanied by a dramatic increase in MMS sensitivity and chromosomal defects visualized by PFGE (Figure 2, A–C). Strikingly, these abnormalities, as well as the intra-S-phase delay observed by fluorescence-activated cell sorting (FACS), could be rescued in cells expressing the *rad53-R605A* allele (Figure 2, D–G). Of importance, the *slx4* mutant bearing the S486A mutation, which encodes a protein that is specifically unable to interact with Dpb11 and promote checkpoint dampening (Ohouo *et al.* 2013), behaved similarly to the full deletion of *SLX4* in our analysis of Rad53 activation, MMS sensitivity, and PFGE (Figure S1). Collectively, these results support the notion that *PPH3* and *SLX4* function in parallel, representing two complementary mechanisms for downregulating Rad53. These two mechanisms and their concerted action seem particularly important for regulating Rad53 signaling following the bypass of replication blocks.

Rad53 hypersignaling in slx4Δ or pph3Δ cells impairs proper cell cycle-dependent regulation of the Mus81-Mms4 nuclease

Replication forks typically bypass MMS-induced replication blocks via template switching mechanisms, resulting in physical linkages between sister chromatids, also known as joint molecules (JMs) (Branzei *et al.* 2008). Processing of these linkages is crucial for chromosome segregation and occurs mainly through two parallel mechanisms, either dissolution via the Sgs1-Top3-Rmi1 complex or resolution via the Mus81-Mms4 structure-specific endonuclease (Hickson and Mankouri 2011; Sarbajna and West 2014). The Mus81-Mms4 pathway is under strict cell cycle regulation, being activated in G_2/M by action of the CDK and Cdc5 kinases and presumably antagonized by DDC-mediated cell cycle arrest (Zhang *et al.* 2009; Szakal and Branzei 2013). Because MMS treatment induces massive amounts of JMs, we raised the possibility that repression of Mus81-Mms4 activation imposed by the strong cell cycle arrest is perhaps a major deleterious effect of Rad53 hyperactivation in *slx4Δ* and *pph3Δ* mutants and could explain why these cells are hypersensitive to MMS. To test the hypothesis that temporal misregulation of Mus81-Mms4 activation accounts for the reason why cells lacking *SLX4* and *PPH3* are hypersensitive to MMS-induced replication blocks, we performed genetic analysis with *sgs1Δ* or *mus81Δ* cells. As cells lacking both *SLX4* and *SGS1* are inviable due to the checkpoint-independent role of Slx4 controlling the activity of the Slx1 nuclease (Fricke and Brill 2003), we utilized the *slx4-S486A* allele that we have previously shown to disrupt the checkpoint dampening function of Slx4 (Ohouo *et al.* 2013). Cells lacking *SGS1* and expressing the *slx4-S486A* allele are viable, but display a significant increase in MMS sensitivity compared to the single mutants. In addition, cells lacking *MUS81* and expressing the *slx4-S486A* mutant display MMS sensitivity similar to the *mus81Δ* single mutant (Figure 3A) (see also Gritenaite *et al.* 2014). As for Pph3, a *pph3Δ sgs1Δ* strain also showed enhanced MMS sensitivity compared to single mutants and deletion of *PPH3* did not significantly increase the sensitivity of *mus81Δ* cells to MMS (Figure 3B). Taken together, these results are consistent with the model in which a major cause of MMS sensitivity in both *pph3Δ* cells and *slx4Δ* cells is related to the inability of these cells to trigger the timely activation of Mus81-Mms4. While Rad53 hypersignaling in these mutants likely has a broad impact on other events linked to cell cycle progression, the fact that these cells are selectively sensitive to MMS suggests that Mus81-Mms4 activation likely becomes the major limiting factor upon extensive accumulation of JMs.

We reasoned that if a crucial role of *PPH3*-dependent or *SLX4*-dependent downregulation of Rad53 signaling is to promote timely Mus81-Mms4 activation, the *rad53-R605A* allele would rescue the MMS sensitivity of either *slx4Δ* or *pph3Δ* cells but not the sensitivity of cells lacking *MUS81*. Indeed, swapping the endogenous copy of *RAD53* for the *rad53-R605A* allele failed to rescue the MMS sensitivity of *mus81Δ*, *mus81Δ pph3Δ*, or *mus81Δ slx4Δ* cells (Figure 3C and Figure S2). Interestingly, while the *rad53-R605A* allele could rescue the strong intra-S delay observed in *mus81Δ pph3Δ slx4Δ* cells (Figure 3D), we could not observe any rescue of the chromosome defects seen by PFGE (Figure 3E). This finding strongly suggests that the chromosome defects seen by PFGE in *slx4Δ* and *pph3Δ* cells are not due to the negative impact of Rad53 signaling on bulk DNA synthesis, but most likely due to the negative impact of Rad53 signaling on the ability of cells to resolve joint chromosomes via Mus81-Mms4 action. This interpretation is consistent with a previous report showing that these MMS-induced chromosomal defects observed by PFGE can be attributed to defective Mus81 action after completion of DNA replication (Saugar *et al.* 2013). Finally, cells lacking both *SGS1* and *MUS81* are inviable (Mullen *et al.* 2001) and *sgs1Δ pph3Δ slx4-S486A* cells display a dramatic hypersensitivity to minimal doses of MMS (Figure 3F), underscoring the key role of PP4 and DAMP for proper regulation of the Mus81-Mms4 pathway. Based on the results presented above, we propose that upon replication blocks that promote extensive template switching events and formation of chromosomal linkages, cells strongly rely on the concerted action of Pph3 and Slx4 to downregulate Rad53 signaling for proper cell cycle progression and timely Mus81-Mms4 activation.

Antagonistic roles of H2A phosphorylation in checkpoint regulation provide insights into the mechanism of coordinated action of Slx4-Rtt107 and Pph3

Upon replication stress, the sensor kinase Mec1 extensively phosphorylates histone H2A at serine 129 (γ-H2A) to form

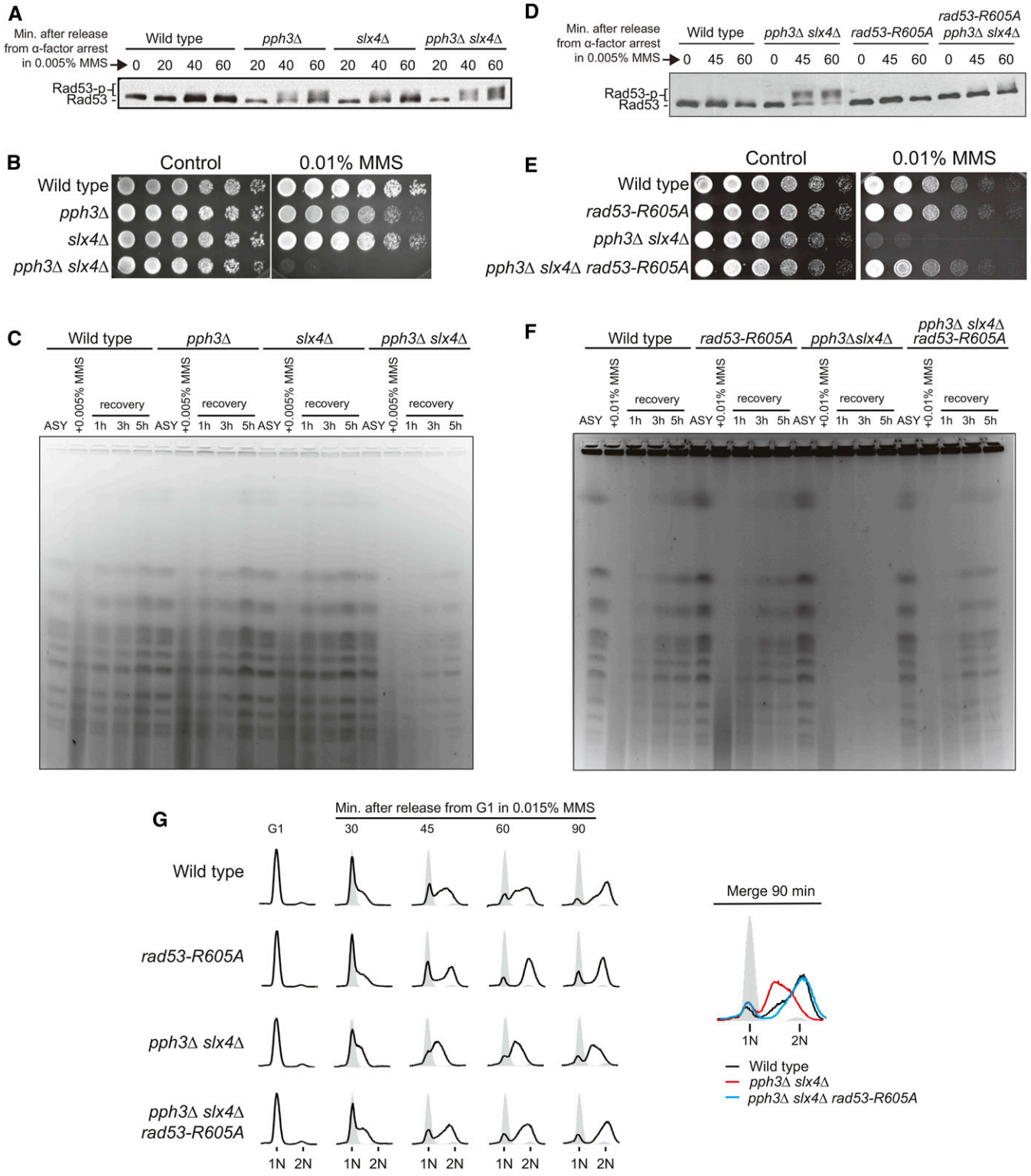

Figure 2 Slx4 and Pph3 function in a complementary manner in the regulation of Rad53 signaling. (A–C) Wild-type, *slx4Δ*, and *pph3Δ* single mutants were compared against a *pph3Δ slx4Δ* strain. (A) Anti-Rad53 immunoblots of wild-type, *slx4Δ*, *pph3Δ*, and *pph3Δ slx4Δ* strains showing Rad53 phosphorylation status after MMS treatment. (B) Serial dilutions assay showing the MMS sensitivity of indicated strains. (C) Analysis of fully replicated chromosomes by PFGE. Asynchronous (ASY) cells were treated with 0.005% MMS for 2 hr and then released in MMS-free medium for up to 5 hr. (D–G) Effect of the *rad53-R605A* allele on (D) Rad53 phosphorylation status, (E) MMS sensitivity, (F) PFGE-monitored chromosomes, and (G) S-phase progression of *pph3Δ slx4Δ* cells. For B and E, assays were performed as described in Figure 1A.

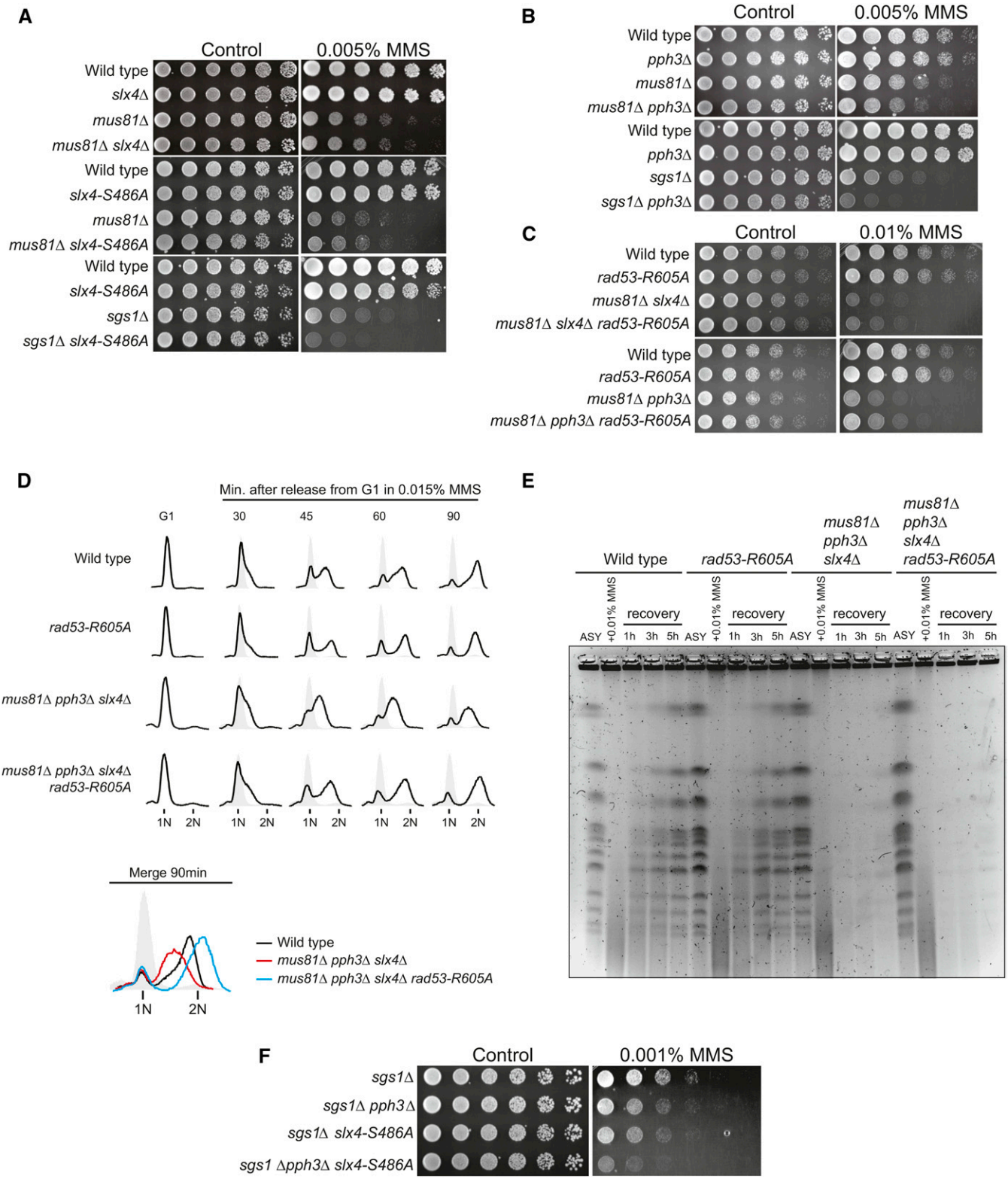

Figure 3 Rad53 hypersignaling in cells lacking *PPH3* and/or *SLX4* converges to misregulation of the Mus81-Mms4 endonuclease. (A and B) Serial dilution assay showing the effect of *MUS81* or *SGS1* deletion on the MMS sensitivity of the indicated strains. (C–E) Effect of the *rad53-R605A* allele on (C) MMS sensitivity, (D) S-phase progression, and (E) PFGE-monitored chromosomes of the indicated strains lacking *MUS81*. In D, cells were released from G_1 arrest in YPD medium containing 0.015% MMS. In E, asynchronous cells were treated with 0.01% MMS for 2 hr and released into MMS-free medium for up to 5 hr. Samples were taken at each indicated time point. (F) Serial dilution assay showing the effect of *SGS1* deletion on the MMS sensitivity of a *pph3Δ slx4-S486A* strain.

a platform of γ-H2A surrounding the site of lesion (Shroff *et al.* 2004; Balint *et al.* 2015). This γ-H2A platform recruits Rad9, via BRCT domains, and therefore contributes to promoting Rad53 activation (Hammet *et al.* 2007; Ohouo *et al.* 2013). Unexpectedly, previous work from the Haber laboratory found that the nonphosphorylatable S129A mutation in H2A does not rescue, but slightly increases, the MMS sensitivity of *pph3Δ* cells (Kim *et al.* 2011). Here, elucidation of the complementary actions of Pph3 and Slx4 provides important insight into the roles of γ-H2A in the response to MMS treatment. As shown in Figure 4A, the *hta-S129A* mutation does not provide any rescue of the MMS sensitivity of *pph3Δ* cells, but confers substantial, albeit incomplete, rescue of *slx4Δ* cells. The apparent antagonistic roles of γ-H2A in each of these mutants may be explained by the fact that the Slx4-Rtt107 complex strictly relies on γ-H2A for recruitment (Balint *et al.* 2015) and enforcement of DAMP (Ohouo *et al.* 2013), whereas Rad9 can be recruited via either γ-H2A or methylated H3K79 (Giannattasio *et al.* 2005; Wysocki *et al.* 2005; Toh *et al.* 2006). A likely scenario is that in the absence of *PPH3* there is an increased dependency on the Slx4-Rtt107 complex for counteracting Rad53 activation, and γ-H2A becomes crucial for checkpoint downregulation, while not essential for checkpoint activation (Rad9 can still be recruited via methylated H3K79). Therefore, *hta-S129A* will mostly result in less checkpoint dampening and increased checkpoint activation in *pph3Δ* cells. On the other hand, in the absence of *SLX4*, as γ-H2A serves mainly for checkpoint activation, *hta-S129A* will lead to reduced checkpoint activation. Indeed, we observed that expression of the *hta-S129A* mutant increased activation of Rad53 in *pph3Δ* cells, but reduced Rad53 activation in *slx4Δ* cells (Figure 4B). Finally, we predicted that elimination of H3K79 methylation, important for Rad9 recruitment but not for Slx4-Rtt107 recruitment, would cause an opposite effect to that of the *hta-S129A* mutation, resulting in rescue of MMS sensitivity of *pph3Δ* cells. To test this idea, we deleted *DOT1*, the methyltransferase responsible for methylation of H3K79 (van Leeuwen *et al.* 2002), in *pph3Δ* cells and in *slx4Δ* cells and monitored MMS sensitivity. As predicted, *dot1Δ* rescued the MMS sensitivity of *pph3Δ* cells as well as of *slx4Δ* cells (Figure 4C). These results elucidate the apparent antagonistic roles of γ-H2A in checkpoint control (Figure 4D) and highlight the elaborate coordination of the actions of Pph3 and Slx4 during the response to MMS. Interestingly, γ-H2A is itself a target of Pph3 (Keogh *et al.* 2006), adding an additional level of complexity to the coordinated action of Pph3 and Slx4-Rtt107.

Slx4-Rtt107 and PP4 function in spatially distinct modes

Single-mutant cells lacking either *PPH3* or *SLX4* display hyperactive Rad53 activation (Figure 1B), revealing that these mechanisms of Rad53 downregulation are not redundant and cannot be fully compensated by each other. We reasoned that DAMP functions in a more localized fashion, as it requires interaction of Slx4-Rtt107 with γ-H2A and the Dpb11 scaffold (Ohouo *et al.* 2013; Cussiol *et al.* 2015), which are both specifically located at sites of lesions (Balint *et al.* 2015). In support of a model in which Slx4-Rtt107 functions at sites of DNA lesions, recent work form the Brown laboratory using ChIP-seq has shown that Slx4-Rtt107 robustly localizes to chromatin as replication forks traverse regions of MMS-alkylated DNA (Balint *et al.* 2015). On the other hand, a previous report on the action of Pph3 in response to DSBs showed that chromatin-bound γ-H2A is not affected by Pph3 action (Keogh *et al.* 2006), suggesting that Pph3 mostly functions on free pools of γ-H2A and, by extension, Rad53. In this scenario, precise downregulation of Rad53 activation would be achieved only through the coordinated local and global actions of Pph3 and Slx4, respectively. Interestingly, while both Slx4 and Pph3 form nuclear foci upon MMS treatment (Figure 5A) (see also Tkach *et al.* 2012), Slx4 and Pph3 foci do not colocalize (Figure 5B), further supporting the model that Pph3 and Slx4 act in spatially distinct manners. Also congruent with this notion, we found that expression of a minimal multi-BRCT-domain (MBD) module, previously shown to strongly reduce Rad53 activation by counteracting the Rad9 adaptor at sites of lesions (Cussiol *et al.* 2015), could fully rescue the MMS sensitivity of cells lacking *SLX4* but not the sensitivity of cells lacking *PPH3* (Figure 5C). In contrast to MBD, the *rad53-R605A* hypomorphic allele can fully rescue the MMS sensitivity of *pph3Δ* cells (see Figure 1E), which suggests that *PPH3* is crucial to deactivate even low levels of activated Rad53 that have diffused from the site of lesion. It is important to mention that the MBD module docks at the lesion site only after an initial bout of Mec1 activation that creates the γ-H2A and phospho-Ddc1 anchoring points for the BRCT domains of Rtt107 and Dpb11, respectively (Cussiol *et al.* 2015). In this manner, some population of active Rad53 would be quickly generated, even upon expression of MBD. But once diffused, active Rad53 molecules would be unable to be properly deactivated in *pph3Δ* cells.

To better spatially define the action of Pph3 and specifically address the question of whether it acts on chromatin or on free pools of histone H2A during replication stress, we used ChIP-seq to monitor γ-H2A, another Pph3 target (Keogh *et al.* 2006). Because γ-H2A can be robustly detected on chromatin, even in the absence of DNA damage (Szilard *et al.* 2010), it provides a convenient substrate to address whether Pph3 acts on chromatin. We performed ChIP-seq analysis of γ-H2A, comparing wild-type, *pph3Δ*, and *slx4Δ* cells in S phase, treated with MMS. Cells were arrested in G_1 with α-factor and then released into S phase in medium containing MMS. As shown in Figure 5, D–F, we could observe accumulation of γ-H2A near early origins of replication (represented by green marks) in wild-type and *slx4Δ* cells, consistent with the idea that H2A is phosphorylated upon movement of replication forks over regions of alkylated DNA, while regions not yet replicated are mostly devoid of strong γ-H2A signal. In cells lacking *PPH3* (Figure 5E) we could not detect preferential accumulation of γ-H2A at those same origin-proximal regions, and the overall detected signal is delocalized and appears across the entire chromosome,

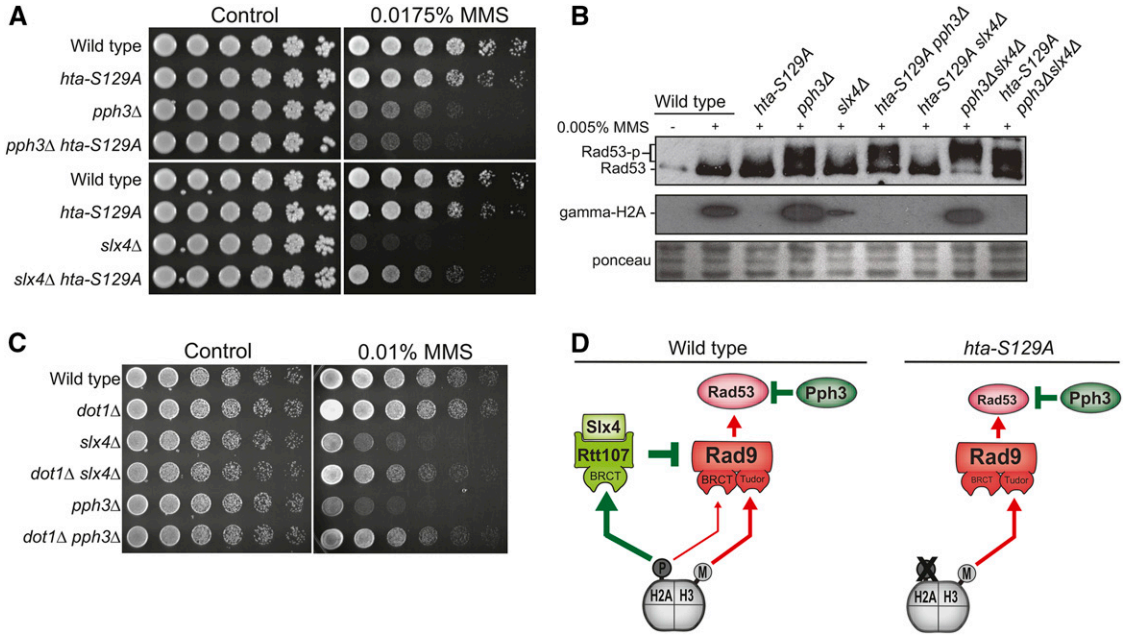

Figure 4 Antagonistic roles for γ-H2A in DDC control. (A and B) Effect of an H2A phospho-mutant (*hta-S129A*) on the MMS sensitivity (A) and Rad53 phosphorylation (B) of *slx4Δ* and *pph3Δ* strains. In B, asynchronous cells were treated with 0.005% MMS for 2 hr and samples were collected. Western blot analyses were performed using anti-Rad53 and anti-γ-H2A antibodies as described in *Material and Methods*. (C) Serial dilution assay showing the effect of *DOT1* deletion on the MMS sensitivity of *slx4Δ* and *pph3Δ* strains. (D) Proposed model conciliating the antagonistic roles of γ-H2A on DDC regulation.

with concurrent accumulation of massive amounts of total γ-H2A (Figure 5I). Of note, the differential accumulation of γ-H2A at early origins in wild-type and *slx4Δ* cells compared with *pph3Δ* cells (Figure 5G) is not due to differences in the replication timing between these strains (Figure 5H). We interpret this result as Pph3 acting mainly on free pools of gamma-H2A, before they are recycled back onto chromatin, consistent with previous work showing that Pph3 does not act on chromatin γ-H2A upon DSB induction (Keogh *et al.* 2006). In summary, the microscopy, genetic, and ChIP data presented above support the model that Pph3 and Slx4 function in spatially distinct manners. Our work here supports the model that Slx4-Rtt107 has a primary role in downregulating Rad53 activation locally, on chromatin, as replication forks bypass lesions, whereas Pph3 likely has a more predominant role in dephosphorylating active Rad53 at diffused nuclear pools (Figure 5J).

Discussion

Upon replication stress, DNA damage checkpoint signaling plays crucial roles in preserving cell viability mainly by protecting the integrity of replication forks, but this benefit comes at the expense of a strong repression of cell cycle progression and DNA synthesis. Mechanisms for termination of checkpoint signaling are therefore required to maintain the proliferative capacity of cells. Using budding yeast as a model system, we show that proper termination of Rad53 signaling following the bypass of replication blocks requires the concerted action of two fundamentally distinct mechanisms for checkpoint downregulation. We find that the Pph3 phosphatase functions in a highly complementary manner to the mechanism of checkpoint dampening mediated by the Slx4-Rtt107 repair scaffolds. Based on our findings, we propose a model in which Slx4-Rtt107 acts locally to counteract Rad53 activation at sites of DNA lesions bypassed by the replication machinery, while Pph3 deactivates pools of Rad53 that have diffused from the site of lesion. The action of both mechanisms is therefore required for full termination of checkpoint signaling triggered by replication blocks.

JM accumulation likely explains why cells lacking PPH3 and/or SLX4 are particularly sensitive to MMS-induced replication stress

MMS is a monofunctional DNA alkylating agent that primarily methylates DNA on N^7-deoxyguanine and N^3-deoxyadenine (Drablos *et al.* 2004), generating adducts that block the progression of DNA polymerases. A distinct feature of MMS-induced replication stress, when compared to HU- or camptothecin (CPT)-induced replication stress, is that DNA adducts generated by MMS are readily bypassed by moving replication forks so DNA synthesis proceeds, albeit slower, and cells eventually replicate their chromosomes in a timely manner, especially with the low doses of MMS used in the experiments presented here. However, because replication fork bypass is achieved through, or results in, template-switching events, completion of replication is accompanied by extensive formation of chromosomal linkages (JMs) (Boiteux and Jinks-Robertson 2013). We speculate that the massive accumulation of JMs in MMS-treated cells is the main reason behind the strong sensitivity of *slx4Δ* and/or *pph3Δ* cells to MMS. Consistent with this notion, checkpoint signaling arrests the cell cycle, preventing activation of

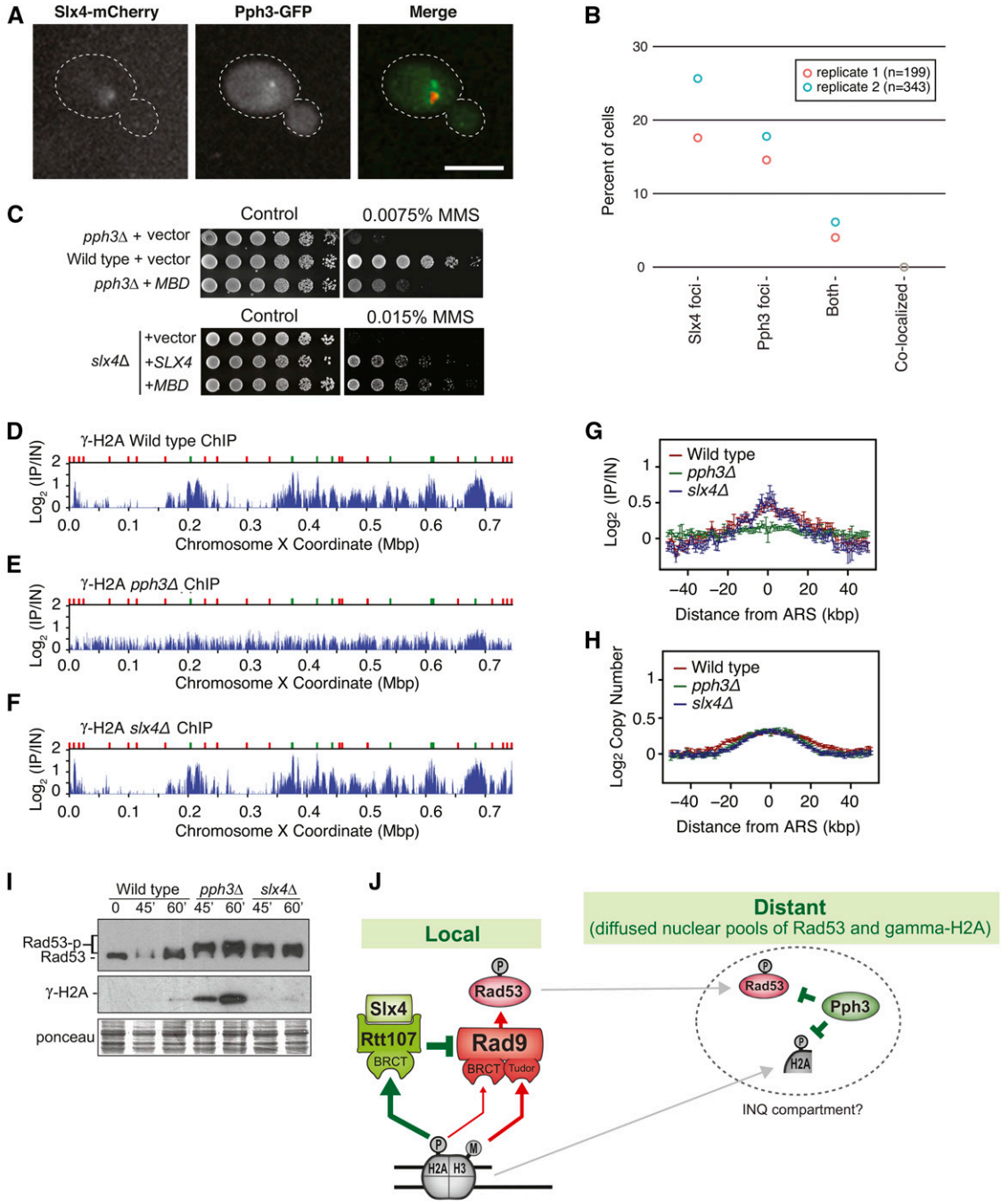

Figure 5 Pph3 and Slx4 function in spatially distinct manners. (A) Representative images showing the intracellular localization of Slx4 and Pph3 proteins. (B) Slx4-yEmCherry and Php3-GFP foci were measured by confocal fluorescence microscopy after MMS treatment. The percentage of cells with Slx4-yEmCherry, Php3-GFP, and both Slx4-yEmCherry/Php3-GFP foci is plotted. (C) Serial dilution assay showing the effect of MBD expression on the MMS sensitivity of the selected strains. *MBD* and *SLX4* were expressed from a *pRS416* plasmid (for details see Table S2) in SC –URA. (D–F) ChIP-seq analysis was performed following synchronous release of wild-type (D), *pph3Δ* (E), and *slx4Δ* (F) cells into S phase in the presence of 0.04% MMS for 60 min. γ-H2A (S129) enrichment scores on chromosome X are shown. Early origins are indicated by green bars and late origins by red bars. (G and H) The median γ-H2A ChIP enrichment scores (G) and replication profiles (H) across 108 early-firing origins, in wild-type, *pph3Δ*, and *slx4Δ* cells, are plotted. (I) Immunoblot showing the status of Rad53 and γ-H2A in wild-type, *pph3Δ*, and *slx4Δ* cells after treatment of G_1 synchronized cultures with α-factor and release into medium containing 0.01% MMS for the indicated time points. (J) Proposed model illustrating how Pph3 and Slx4 coordinate Rad53 downregulation in spatially distinct manners.

Mus81-Mms4 (Szakal and Branzei 2013), the main nuclease involved in resolution of JMs, and deletion of *SLX4* and/or *PPH3* does not further sensitize *mus81Δ* cells to MMS treatment (Figure 3C). Interestingly, drugs that result in other types of replication stress that do not induce extensive JM formation also lead to cell cycle arrest, but do not cause growth sensitivity

in *slx4Δ* and/or *pph3Δ* cells. We speculate that while other cell cycle-dependent events are probably executable with low levels of CDK and/or Cdc5 activity, JM resolution requires robust and timely activation of these cell cycle kinases. In addition, it is possible that if activation of Mus81-Mms4 is delayed for too long, aberrant JM processing can compromise chromosomal integrity and cell viability.

Transitioning from fork protection to JM resolution

In our proposed model (Figure 5J), Rad53 is rapidly activated as replication forks encounter MMS-induced DNA adducts. Rad53 activation in response to MMS treatment is mostly mediated by the Rad9 adaptor (Ohouo *et al.* 2013) and is thought to occur proximal to replication fork regions mainly to protect the integrity of replication forks. This fork protection function likely relies on the local action of Rad53 in inhibiting nucleases, such as Exo1, from processing fork structures (Morin *et al.* 2008). In addition, the global action of Rad53 in inhibiting origin firing, increasing dNTP levels, and halting cell cycle progression supposedly has an overall positive impact on fork integrity. However, as forks bypass the lesions and JMs are formed, the importance of fork protection transitions to JM processing. Such transition requires downregulation of Rad53 signaling mainly because resolution of JMs via Mus81-Mms4 is tightly coupled to activation of the cell cycle kinases Cdc5 and CDK, which are thought to be inhibited by checkpoint signaling. Of importance, the mechanism by which Rad53 may supposedly inhibit Cdc5 and CDK in budding yeast remains incompletely understood. Taken together, our model implies that, in a first moment, *slx4Δ* and *pph3Δ* cells suffer from a recovery defect due to the inability to properly downregulate Rad53 after the bypass of replication blocks. Given the strong dependency on Mus81 to resolve MMS-induced JMs, the recovery defect results in a subsequent repair defect due to hyper-inhibition of Mus81-Mms4.

Rad53 as a mobile kinase

The mechanism underlying Rad53 activation presupposes that it is activated in a localized manner at sites of DNA lesions (Alcasabas *et al.* 2001; Gilbert *et al.* 2001). The fact that Rad53 plays roles in signaling responses that occur distant from sites of lesions, such as transcription and cell cycle control, is consistent with the notion that Rad53 is a highly mobile kinase. While the well-established mode of Rad53 activation following replication stress involves recruitment of Rad53 close to the sensor kinase Mec1 at sites of RPA-coated ssDNA, Rad53 seems to rapidly diffuse from these sites, as inferred by the following negative or indirect observations: (1) Microscopic analysis showed that Rad53 foci are faint and tend to rapidly dissipate (Lisby *et al.* 2004); (2) ChIP experiments have not been able to robustly detect Rad53 on chromatin and a weak Rad53 signal has been detected at replicating regions only after treatment with protein–protein cross-linking agents (Katou *et al.* 2003); and (3) CHK2, the mammalian homolog of Rad53, has been shown to form a pan-nuclear distribution throughout the nucleus minutes after DNA double-strand break formation, and forced immobilization of CHK2 at the DNA lesion site affects phosphorylation of CHK2 targets (Lukas *et al.* 2003). The realization that Rad53 is a highly mobile kinase has crucial implications for understanding how it is deactivated and is congruent with our finding of two complementary modes of Rad53 deactivation, one acting locally to prevent new Rad53 molecules from being activated and another acting globally to deactivate pools of active Rad53 that have diffused form the site of lesion. Interestingly, a recent report has shown that Pph3 foci colocalize with an intranuclear quality control (INQ) compartment proposed to be involved in the recovery from genotoxic stress (Gallina *et al.* 2015). It is tempting to speculate that global pools of active Rad53 and phosphorylated H2A are eventually sequestered into these INQ compartments for dephosphorylation.

A spatial model for termination of Rad53 signaling following the bypass of DNA lesions

We propose a model in which the proper downregulation of Rad53 signaling requires the concerted action of the Slx4-Rtt107 scaffold and the PP4 phosphatase. The Slx4-Rtt107 complex functions at sites of lesions to prevent continued Rad53 activation via the Rad9 adaptor. As previously reported, this is achieved by the ability of Slx4-Rtt107 to interact with the Dpb11 scaffold and lesion-specific phospho-sites in histone H2A and on the Ddc1 component of the 9-1-1 complex. However, this DAMP mechanism is unable to deal with the pools of activated Rad53 that have diffused from the site of lesion. In this manner, proper termination of Rad53 signaling also requires the action of the PP4 phosphatase, which should presumably be capable of deactivating the pools of Rad53 that have diffused. Consistent with this notion, localization data reveal that Pph3 is evenly distributed throughout the nucleoplasm or at the specialized INQ compartment (Gallina *et al.* 2015) and ChIP data show that the γ-H2A is likely not dephosphorylated by Pph3 on chromatin, but in the nucleoplasm as it is being recycled back to chromatin. Interestingly, the recent finding that Pph3 physically interacts with Mec1 (Hustedt *et al.* 2015) raises new possibilities as to how Pph3 may strategically localize to more efficiently target the pools of Rad53 emanating from sites of activation.

Overall, the proposed model for the spatial coordination of Rad53 deactivation is supported by the genetic, biochemical, and cell biological data presented here. Mus81 action requires an increase in Cdc5 and CDK activity, and it is plausible that both of these kinases, similar to Rad53, are also highly diffused throughout the nucleus. It is tempting to speculate that Cdc5 itself may be somehow subjected to repression by global pools of activated Rad53, highlighting the importance of full deactivation of the complete pool of Rad53 for proper cell cycle progression and Mus81 activation. It will be interesting to test whether the human PP4 phosphatase also acts on diffused pools of checkpoint kinases and in coordination with more localized mechanisms of checkpoint downregulation to properly regulate cell cycle progression and timely processing of repair intermediates, such as JMs.

Acknowledgments

We thank James Haber and José Tercero for comments and suggestions. We thank Achille Pellicioli for the α-Rad53 antibody. This work was supported by a grant to M.B.S. from the National Institutes of Health (R01-GM097272), a grant to G.W.B. from the Canadian Cancer Society Research Institute (702310), a grant to G.W.B. from the Canadian Institutes of Health Research (MOP-79368), and a grant to Z.Z. from the Natural Sciences and Engineering Research Council of Canada (327612).

Literature Cited

Alcasabas, A. A., A. J. Osborn, J. Bachant, F. Hu, P. J. Werler *et al.*, 2001 Mrc1 transduces signals of DNA replication stress to activate Rad53. Nat. Cell Biol. 3: 958–965.

Bähler, J., J. Q. Wu, M. S. Longtine, N. G. Shah, A. McKenzie *et al.*, 1998 Heterologous modules for efficient and versatile PCR-based gene targeting in *Schizosaccharomyces pombe*. Yeast 14: 943–951.

Balint, A., T. Kim, D. Gallo, J. R. Cussiol, F. M. Bastos de Oliveira *et al.*, 2015 Assembly of Slx4 signaling complexes behind DNA replication forks. EMBO J. 34: 2182–2197.

Boiteux, S., and S. Jinks-Robertson, 2013 DNA repair mechanisms and the bypass of DNA damage in *Saccharomyces cerevisiae*. Genetics 193: 1025–1064.

Branzei, D., and M. Foiani, 2009 The checkpoint response to replication stress. DNA Repair 8: 1038–1046.

Branzei, D., and M. Foiani, 2010 Maintaining genome stability at the replication fork. Nat. Rev. Mol. Cell Biol. 11: 208–219.

Branzei, D., F. Vanoli, and M. Foiani, 2008 SUMOylation regulates Rad18-mediated template switch. Nature 456: 915–920.

Chang, M., M. Bellaoui, C. Boone, and G. W. Brown, 2002 A genome-wide screen for methyl methanesulfonate-sensitive mutants reveals genes required for S phase progression in the presence of DNA damage. Proc. Natl. Acad. Sci. USA 99: 16934–16939.

Cussiol, J. R., C. M. Jablonowski, A. Yimit, G. W. Brown, and M. B. Smolka, 2015 Dampening DNA damage checkpoint signalling via coordinated BRCT domain interactions. EMBO J. 34: 1704–1717.

Davidson, M. B., Y. Katou, A. Keszthelyi, T. L. Sing, T. Xia *et al.*, 2012 Endogenous DNA replication stress results in expansion of dNTP pools and a mutator phenotype. EMBO J. 31: 895–907.

Drablos, F., E. Feyzi, P. A. Aas, C. B. Vaagbo, B. Kavli *et al.*, 2004 Alkylation damage in DNA and RNA–repair mechanisms and medical significance. DNA Repair 3: 1389–1407.

Fricke, W. M., and S. J. Brill, 2003 Slx1-Slx4 is a second structure-specific endonuclease functionally redundant with Sgs1-Top3. Genes Dev. 17: 1768–1778.

Gallina, I., C. Colding, P. Henriksen, P. Beli, K. Nakamura *et al.*, 2015 Cmr1/WDR76 defines a nuclear genotoxic stress body linking genome integrity and protein quality control. Nat. Commun. 6: 6533.

Giannattasio, M., F. Lazzaro, P. Plevani, and M. Muzi-Falconi, 2005 The DNA damage checkpoint response requires histone H2B ubiquitination by Rad6-Bre1 and H3 methylation by Dot1. J. Biol. Chem. 280: 9879–9886.

Gietz, D., S. A. Jean, R. A. Woods, and R. H. Schiestl, 1992 Improved method for high efficiency transformation of intact yeast cells. Nucleic Acids Res. 20: 1425.

Gilbert, C. S., C. M. Green, and N. F. Lowndes, 2001 Budding yeast Rad9 is an ATP-dependent Rad53 activating machine. Mol. Cell 8: 129–136.

Granata, M., F. Lazzaro, D. Novarina, D. Panigada, F. Puddu *et al.*, 2010 Dynamics of Rad9 chromatin binding and checkpoint function are mediated by its dimerization and are cell cycle-regulated by CDK1 activity. PLoS Genet. 6: e1001047.

Grenon, M., C. Gilbert, and N. F. Lowndes, 2001 Checkpoint activation in response to double-strand breaks requires the Mre11/Rad50/Xrs2 complex. Nat. Cell Biol. 3: 844–847.

Grenon, M., T. Costelloe, S. Jimeno, A. O'Shaughnessy, J. Fitzgerald *et al.*, 2007 Docking onto chromatin via the *Saccharomyces cerevisiae* Rad9 Tudor domain. Yeast 24: 105–119.

Gritenaite, D., L. N. Princz, B. Szakal, S. C. Bantele, L. Wendeler *et al.*, 2014 A cell cycle-regulated Slx4-Dpb11 complex promotes the resolution of DNA repair intermediates linked to stalled replication. Genes Dev. 28: 1604–1619.

Hammet, A., C. Magill, J. Heierhorst, and S. P. Jackson, 2007 Rad9 BRCT domain interaction with phosphorylated H2AX regulates the G1 checkpoint in budding yeast. EMBO Rep. 8: 851–857.

Hennessy, K. M., A. Lee, E. Chen, and D. Botstein, 1991 A group of interacting yeast DNA replication genes. Genes Dev. 5: 958–969.

Hickson, I. D., and H. W. Mankouri, 2011 Processing of homologous recombination repair intermediates by the Sgs1-Top3-Rmi1 and Mus81-Mms4 complexes. Cell Cycle 10: 3078–3085.

Hustedt, N., A. Seeber, R. Sack, M. Tsai-Pflugfelder, B. Bhullar *et al.*, 2015 Yeast PP4 interacts with ATR homolog Ddc2-Mec1 and regulates checkpoint signaling. Mol. Cell 57: 273–289.

Kastan, M. B., and J. Bartek, 2004 Cell-cycle checkpoints and cancer. Nature 432: 316–323.

Katou, Y., Y. Kanoh, M. Bando, H. Noguchi, H. Tanaka *et al.*, 2003 S-phase checkpoint proteins Tof1 and Mrc1 form a stable replication-pausing complex. Nature 424: 1078–1083.

Keogh, M. C., J. A. Kim, M. Downey, J. Fillingham, D. Chowdhury *et al.*, 2006 A phosphatase complex that dephosphorylates gammaH2AX regulates DNA damage checkpoint recovery. Nature 439: 497–501.

Kim, J.-A. A., W. M. Hicks, J. Li, S. Y. Tay, and J. E. Haber, 2011 Protein phosphatases Pph3, Ptc2, and Ptc3 play redundant roles in DNA double-strand break repair by homologous recombination. Mol. Cell. Biol. 31: 507–516.

Koboldt, D. C., Q. Zhang, D. E. Larson, D. Shen, M. D. McLellan *et al.*, 2012 VarScan 2: somatic mutation and copy number alteration discovery in cancer by exome sequencing. Genome Res. 22: 568–576.

Leroy, C., S. E. Lee, M. B. Vaze, F. Ochsenbien, R. Guerois *et al.*, 2003 PP2C phosphatases Ptc2 and Ptc3 are required for DNA checkpoint inactivation after a double-strand break. Mol. Cell 11: 827–835.

Lisby, M., J. H. Barlow, R. C. Burgess, and R. Rothstein, 2004 Choreography of the DNA damage response: spatiotemporal relationships among checkpoint and repair proteins. Cell 118: 699–713.

Longtine, M. S., A. McKenzie, 3rd, D. J. Demarini, N. G. Shah, A. Wach *et al.*, 1998 Additional modules for versatile and economical PCR-based gene deletion and modification in *Saccharomyces cerevisiae*. Yeast 14: 953–961.

Lukas, C., J. Falck, J. Bartkova, J. Bartek, and J. Lukas, 2003 Distinct spatiotemporal dynamics of mammalian checkpoint regulators induced by DNA damage. Nat. Cell Biol. 5: 255–260.

Morin, I., H. P. Ngo, A. Greenall, M. K. Zubko, N. Morrice *et al.*, 2008 Checkpoint-dependent phosphorylation of Exo1 modulates the DNA damage response. EMBO J. 27: 2400–2410.

Mullen, J. R., V. Kaliraman, S. S. Ibrahim, and S. J. Brill, 2001 Requirement for three novel protein complexes in the absence of the Sgs1 DNA helicase in *Saccharomyces cerevisiae*. Genetics 157: 103–118.

Myung, K., C. Chen, and R. D. Kolodner, 2001 Multiple pathways cooperate in the suppression of genome instability in *Saccharomyces cerevisiae*. Nature 411: 1073–1076.

O'Neill, B. M., S. J. Szyjka, E. T. Lis, A. O. Bailey, J. R. Yates, 3rd *et al.*, 2007 Pph3-Psy2 is a phosphatase complex required for Rad53 dephosphorylation and replication fork restart during recovery from DNA damage. Proc. Natl. Acad. Sci. USA 104: 9290–9295.

Ohouo, P. Y., and M. B. Smolka, 2012 The many roads to checkpoint activation. Cell Cycle 11: 4495.

Ohouo, P. Y., F. M. Bastos de Oliveira, Y. Liu, C. J. Ma, and M. B. Smolka, 2013 DNA-repair scaffolds dampen checkpoint signalling by counteracting the adaptor Rad9. Nature 493: 120–124.

Pellicioli, A., and M. Foiani, 2005 Signal transduction: how Rad53 kinase is activated. Curr. Biol. 15: R769–R771.

Pellicioli, A., C. Lucca, G. Liberi, F. Marini, M. Lopes *et al.*, 1999 Activation of Rad53 kinase in response to DNA damage and its effect in modulating phosphorylation of the lagging strand DNA polymerase. EMBO J. 18: 6561–6572.

Pfander, B., and J. F. Diffley, 2011 Dpb11 coordinates Mec1 kinase activation with cell cycle-regulated Rad9 recruitment. EMBO J. 30: 4897–4907.

Puddu, F., M. Granata, L. Di Nola, A. Balestrini, G. Piergiovanni *et al.*, 2008 Phosphorylation of the budding yeast 9–1-1 complex is required for Dpb11 function in the full activation of the UV-induced DNA damage checkpoint. Mol. Cell. Biol. 28: 4782–4793.

Roberts, T. M., M. S. Kobor, S. A. Bastin-Shanower, M. Ii, S. A. Horte *et al.*, 2006 Slx4 regulates DNA damage checkpoint-dependent phosphorylation of the BRCT domain protein Rtt107/Esc4. Mol. Biol. Cell 17: 539–548.

Rouse, J., 2009 Control of genome stability by Slx protein complexes. Biochem. Soc. Trans. 37: 495–510.

Sanchez, Y., B. A. Desany, W. J. Jones, Q. Liu, B. Wang *et al.*, 1996 Regulation of *RAD53* by the *ATM*-like kinases *MEC1* and *TEL1* in yeast cell cycle checkpoint pathways. Science 271: 357–360.

Santocanale, C., and J. F. Diffley, 1998 A Mec1- and Rad53-dependent checkpoint controls late-firing origins of DNA replication. Nature 395: 615–618.

Sarbajna, S., and S. C. West, 2014 Holliday junction processing enzymes as guardians of genome stability. Trends Biochem. Sci. 39: 409–419.

Saugar, I., M. V. Vazquez, M. Gallo-Fernandez, M. A. Ortiz-Bazan, M. Segurado *et al.*, 2013 Temporal regulation of the Mus81-Mms4 endonuclease ensures cell survival under conditions of DNA damage. Nucleic Acids Res. 41: 8943–8958.

Schwartz, M. F., J. K. Duong, Z. Sun, J. S. Morrow, D. Pradhan *et al.*, 2002 Rad9 phosphorylation sites couple Rad53 to the *Saccharomyces cerevisiae* DNA damage checkpoint. Mol. Cell 9: 1055–1065.

Shroff, R., A. Arbel-Eden, D. Pilch, G. Ira, and W. M. Bonner, 2004 Distribution and dynamics of chromatin modification induced by a defined DNA double-strand break. Curr. Biol. 14: 1703–1711.

Sun, Z., D. S. Fay, F. Marini, M. Foiani, and D. F. Stern, 1996 Spk1/Rad53 is regulated by Mec1-dependent protein phosphorylation in DNA replication and damage checkpoint pathways. Genes Dev. 10: 395–406.

Sun, Z., J. Hsiao, D. S. Fay, and D. F. Stern, 1998 Rad53 FHA domain associated with phosphorylated Rad9 in the DNA damage checkpoint. Science 281: 272–274.

Sweeney, F. D., F. Yang, A. Chi, J. Shabanowitz, D. F. Hunt *et al.*, 2005 *Saccharomyces cerevisiae* Rad9 acts as a Mec1 adaptor to allow Rad53 activation. Curr. Biol. 15: 1364–1375.

Szakal, B., and D. Branzei, 2013 Premature Cdk1/Cdc5/Mus81 pathway activation induces aberrant replication and deleterious crossover. EMBO J. 32: 1155–1167.

Szilard, R. K., P. E. Jacques, L. Laramee, B. Cheng, S. Galicia *et al.*, 2010 Systematic identification of fragile sites via genome-wide location analysis of gamma-H2AX. Nat. Struct. Mol. Biol. 17: 299–305.

Szyjka, S. J., J. G. Aparicio, C. J. Viggiani, S. Knott, W. Xu *et al.*, 2008 Rad53 regulates replication fork restart after DNA damage in *Saccharomyces cerevisiae*. Genes Dev. 22: 1906–1920.

Tkach, J. M., A. Yimit, A. Y. Lee, M. Riffle, M. Costanzo *et al.*, 2012 Dissecting DNA damage response pathways by analysing protein localization and abundance changes during DNA replication stress. Nat. Cell Biol. 14: 966–976.

Toh, G. W., A. M. O'Shaughnessy, S. Jimeno, I. M. Dobbie, M. Grenon *et al.*, 2006 Histone H2A phosphorylation and H3 methylation are required for a novel Rad9 DSB repair function following checkpoint activation. DNA Repair 5: 693–703.

van Leeuwen, F., P. R. Gafken, and D. E. Gottschling, 2002 Dot1p modulates silencing in yeast by methylation of the nucleosome core. Cell 109: 745–756.

Weinert, T. A., and L. H. Hartwell, 1988 The *RAD9* gene controls the cell cycle response to DNA damage in *Saccharomyces cerevisiae*. Science 241: 317–322.

Wysocki, R., A. Javaheri, S. Allard, F. Sha, J. Cote *et al.*, 2005 Role of Dot1-dependent histone H3 methylation in G1 and S phase DNA damage checkpoint functions of Rad9. Mol. Cell. Biol. 25: 8430–8443.

Zegerman, P., and J. F. Diffley, 2010 Checkpoint-dependent inhibition of DNA replication initiation by Sld3 and Dbf4 phosphorylation. Nature 467: 474–478.

Zhang, T., S. Nirantar, H. H. Lim, I. Sinha, and U. Surana, 2009 DNA damage checkpoint maintains Cdh1 in an active state to inhibit anaphase progression. Dev. Cell 17: 541–551.

Zhao, X., A. Chabes, V. Domkin, L. Thelander, and R. Rothstein, 2001 The ribonucleotide reductase inhibitor Sml1 is a new target of the Mec1/Rad53 kinase cascade during growth and in response to DNA damage. EMBO J. 20: 3544–3553.

Zhou, Z., and S. J. Elledge, 1993 *DUN1* encodes a protein kinase that controls the DNA damage response in yeast. Cell 75: 1119–1127.

Zou, L., and S. J. Elledge, 2003 Sensing DNA damage through ATRIP recognition of RPA-ssDNA complexes. Science 300: 1542–1548.

Communicating editor: N. M. Hollingsworth

GENETICS

Supporting Information
www.genetics.org/lookup/suppl/doi:10.1534/genetics.115.181479/-/DC1

Termination of Replication Stress Signaling via Concerted Action of the Slx4 Scaffold and the PP4 Phosphatase

Carolyn M. Jablonowski, José R. Cussiol, Susannah Oberly, Askar Yimit, Attila Balint, TaeHyung Kim, Zhaolei Zhang, Grant W. Brown, and Marcus B. Smolka

DOI: 10.1534/genetics.115.181479

Figure S1

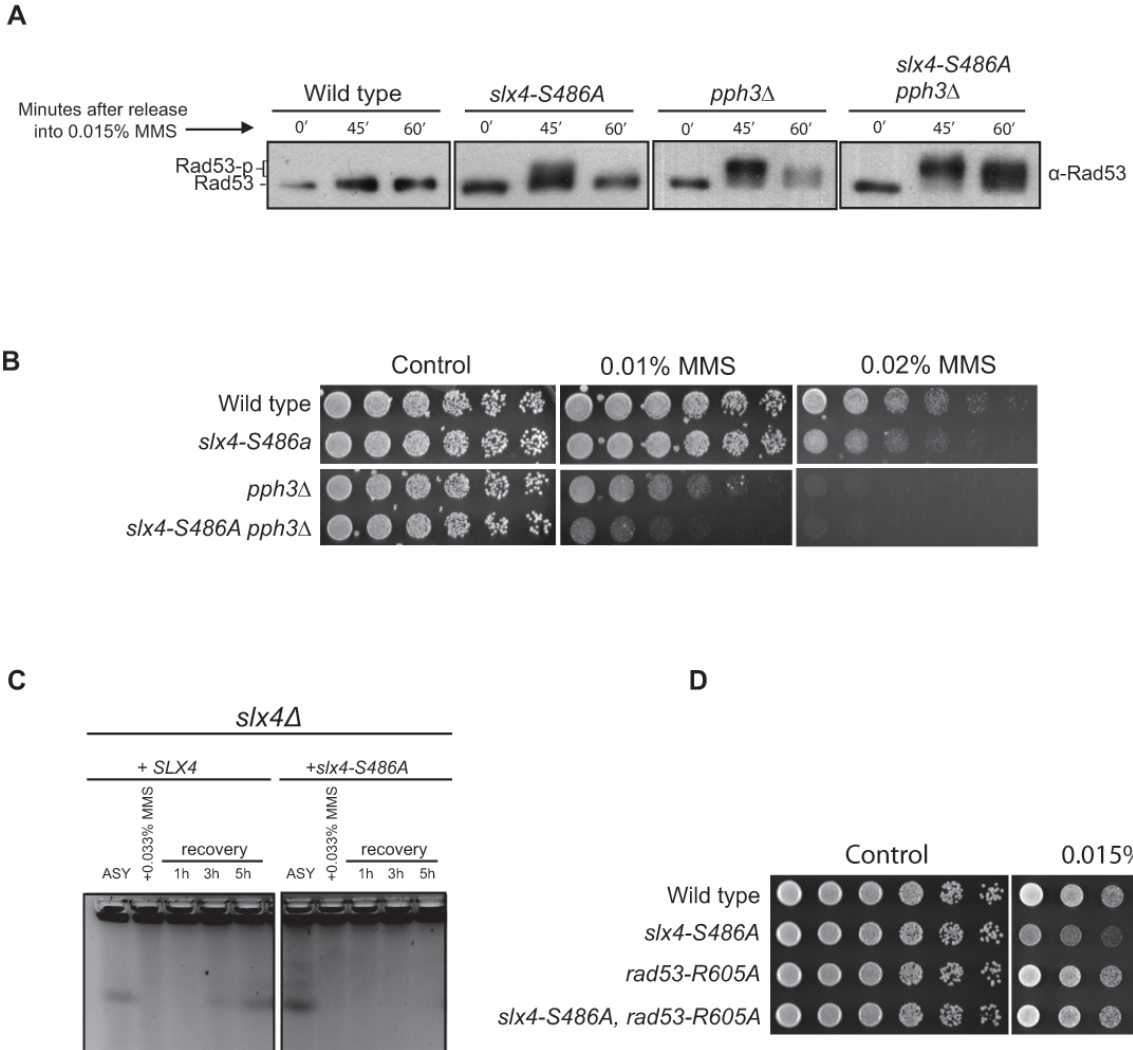
A
Minutes after release into 0.015% MMS
Wild type
slx4-S486A
pph3Δ
slx4-S486A pph3Δ
0′ 45′ 60′
Rad53-p
Rad53
α-Rad53
B
Control
0.01% MMS
0.02% MMS
Wild type
slx4-S486a
pph3Δ
slx4-S486A pph3Δ
C
slx4Δ
+ SLX4
+slx4-S486A
ASY
+0.033% MMS
recovery
1h 3h 5h
D
Control
0.015% MMS
Wild type
slx4-S486A
rad53-R605A
slx4-S486A, rad53-R605A

Figure S1 The *slx4-S486A* mutant phenocopies cells lacking *SLX4* in the response to MMS-induced replication stress. (A) Anti-Rad53 immunoblots of WT, *slx4-S486A*, *pph3Δ* and *pph3Δ slx4-S486A* strains showing Rad53 phosphorylation status after MMS treatment. Experiment was performed as described in Figure 1B. (B) Serial dilution assays showing the effect of MMS treatment upon the sensitivity of wild type, *slx4-S486A*, *pph3Δ* and *pph3Δ slx4-S486A* strains. Four-fold serial dilutions were spotted on YPD plates and grown for 2–3 days at 30°C. (C) Analysis of fully replicated chromosomes measured by PFGE in wild type and *slx4-S486A* strains. Asynchronous (ASY) cells were treated with 0.033% MMS for 3 hours and then released in MMS-free media at different time points. (D) Serial dilution assay showing the effect of a hypomorphic *RAD53* allele (*rad53-R605A*) on MMS sensitivity of wild type and *slx4-S486A* strains.

Figure S2

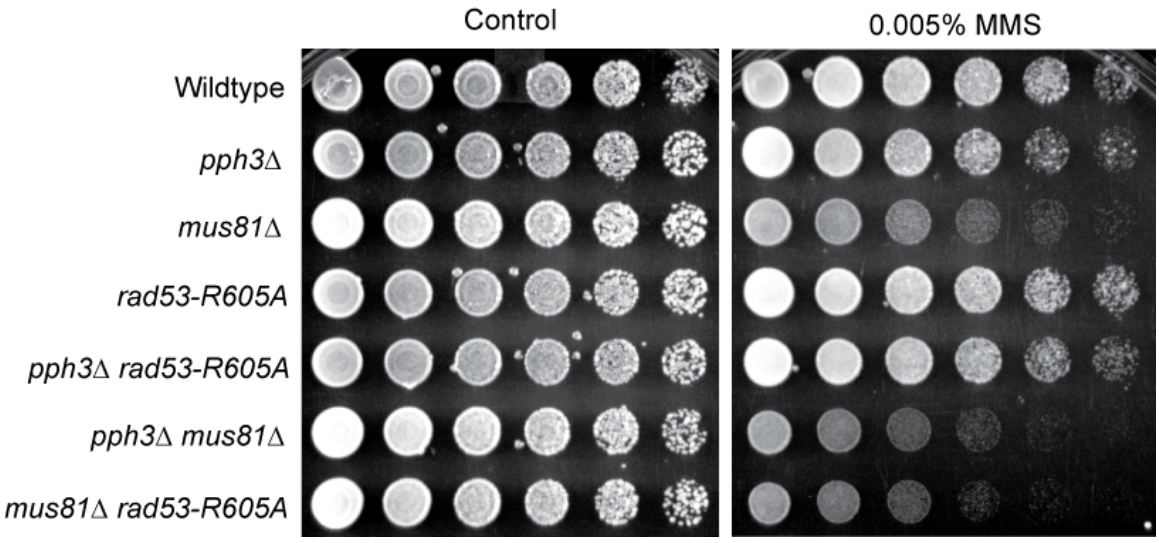
Control
0.005% MMS
Wildtype
pph3Δ
mus81Δ
rad53-R605A
pph3Δ rad53-R605A
pph3Δ mus81Δ
mus81Δ rad53-R605A

Figure S2 Effect of the presence of the *rad53-R605A* allele on the MMS sensitivity of indicated strains lacking. Four-fold serial dilutions were spotted on YPD plates and grown for 2–3 days at 30°C.

Tables S1-S2

Available for download as Excel files at www.genetics.org/lookup/suppl/doi:10.1534/genetics.115.181479/-/DC1

Table S1. *S. cerevisiae* strains used in this study.

Table S2. Plasmids used in this study.